J Biol Inorg Chem (2009) 14:209–217
DOI 10.1007/s00775-008-0439-7

ORIGINAL PAPER

Reversible two-step unfolding of heme–human serum albumin: a ^{1}H-NMR relaxometric and circular dichroism study

Gabriella Fanali · Giampiero De Sanctis · Magda Gioia · Massimo Coletta · Paolo Ascenzi · Mauro Fasano

Received: 28 May 2008 / Accepted: 29 September 2008 / Published online: 21 October 2008

Abstract Human serum albumin (HSA) participates in heme scavenging, the bound heme turning out to be a reactivity center and a powerful spectroscopic probe. Here, the reversible unfolding of heme–HSA has been investigated by ^{1}H-NMR relaxometry, circular dichroism, and absorption spectroscopy. In the presence of 6 equiv of myristate (thus fully saturating all available fatty acid binding sites in serum heme–albumin), 1.0 M guanidinium chloride induces some unfolding of heme–HSA, leading to the formation of a folding intermediate; this species is characterized by increased relaxivity and enhanced dichroism signal in the Soret region, suggesting a more compact heme pocket conformation. Heme binds to the folding intermediate with $K_d = (1.2 \pm 0.1) \times 10^{-6}$ M. In the absence of myristate, the conformation of the folding intermediate state is destabilized and heme binding is weakened [$K_d = (3.4 \pm 0.1) \times 10^{-5}$ M]. Further addition of guanidinium chloride (up to 5 M) brings about the usual denaturation process. In conclusion, myristate protects HSA from unfolding, stabilizing a folding intermediate state in equilibrium with the native and the fully unfolded protein, envisaging a two-step unfolding pathway for heme–HSA in the presence of myristate.

Keywords Circular dichroism · ^{1}H-NMR relaxometry · Heme–human serum albumin · Guanidinium chloride · Folding intermediate state

Abbreviations

B	Basic
CD	Circular dichroism
F	Fast migrating
FA	Fatty acid
GnCl	Guanidinium chloride
HSA	Human serum albumin
N	Neutral

Introduction

Human serum albumin (HSA), a nonglycosylated 66-kDa protein consisting of 585 amino acids, is the most abundant

G. Fanali · M. Fasano (✉)
Dipartimento di Biologia Strutturale e Funzionale,
and Centro di Neuroscienze,
Università dell'Insubria,
Via Alberto da Giussano 12,
21052 Busto Arsizio (VA), Italy
e-mail: mauro.fasano@uninsubria.it

G. De Sanctis
Dipartimento di Biologia Molecolare,
Cellulare ed Animale,
Università di Camerino,
Via Gentile da Varano III s.n.c.,
62032 Camerino (MC), Italy

M. Gioia · M. Coletta
Dipartimento di Medicina Sperimentale e Scienze Biochimiche,
Università di Roma "Tor Vergata",
Via Montpellier 1,
00133 Rome, Italy

P. Ascenzi
Istituto Nazionale per le Malattie Infettive
IRCCS "Lazzaro Spallanzani",
Via Portuense 292,
00149 Rome, Italy

P. Ascenzi
Laboratorio Interdisciplinare di Microscopia Elettronica,
Università Roma Tre,
Via della Vasca Navale 79,
00146 Rome, Italy

protein in plasma. The modular three-domain structure of HSA, which probably arises from a divergent evolution of a degenerated ancestral gene followed by fusion events, is made by two flexible interdomain helices linking domains I–II and II–III, respectively. Each domain is formed by two separate subdomains (named A and B), connected by a random coil (Fig. 1) [1–5].

HSA is a well-known plasma carrier, characterized by an extraordinary ligand binding capacity, being able to interact with amino acids, hormones, metal ions, bilirubin, and drugs. Furthermore, HSA binds up to 7 equiv of long-chain fatty acids (FAs; such as myristate) at multiple binding sites with different affinity (Fig. 1). In sites FA1–FA5 the carboxylate moiety of FAs is anchored by electrostatic/polar interactions; in contrast, sites FA6 and FA7 do not display clear evidence of polar interactions that keep in place the carboxylate head of the FA, thus suggesting that sites FA6 and FA7 are low-affinity FA binding sites [3, 4, 6–10]. One of the FA binding sites (FA1) has evolved to selectively bind heme with high affinity ($K_d = 1.0 \times 10^{-8}$ M [11]) with the tetrapyrrole ring arranged in a D-shaped cavity limited by Tyr138 and Tyr161 residues that provide π–π stacking interaction with the porphyrin and supply a donor oxygen (from Tyr161) for the Fe(III) heme iron [10–14]. In turn, heme binding to HSA endows the protein with heme-based reactivity [4, 15] and spectroscopic properties [16–21].

Myristate, binding to all FA sites, competes with heme in FA1 and at the same time modulates the neutral (N) to basic (B) transition and stabilizes the binding of heme with an overall twofold increase of K_d [21]. Binding of FAs to HSA is known to determine a conformational change in the protein structure [3, 5, 13, 20].

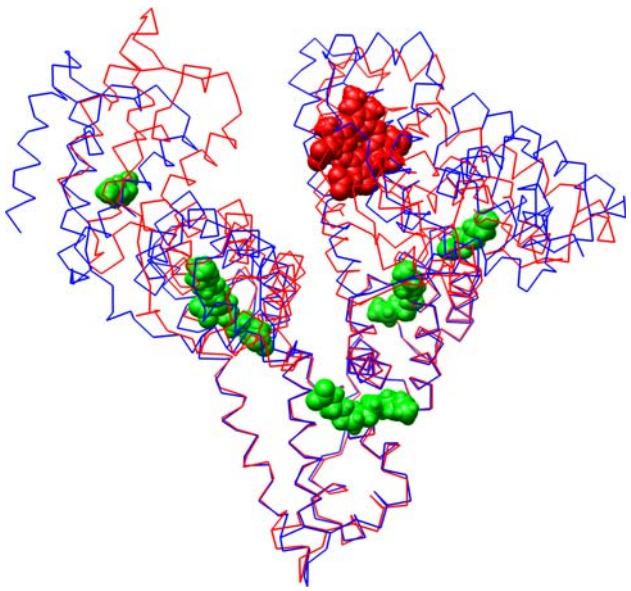

Fig. 1 Three-dimensional structures of human serum albumin (HSA) in the absence (Protein Data Bank entry 1AO6 [39], in *red*) and in the presence (Protein Data Bank entry 1O9X [12], in *blue*) of heme and myristate. Heme (*red*) and myristate ions (*green*) are rendered as space-fill. For details, see the text

HSA structure undergoes pH- and ligand-dependent reversible conformational transition(s). Between pH 2.7 and 4.3 and in the absence of ligands, HSA displays the fast-migrating (F) form, characterized by increased viscosity, low solubility, and a significant loss in helical content. Between pH 4.3 and 8.0 and in the absence of ligands, HSA displays the N form, which is characterized by the typical heart-shaped structure and increased affinity for some ligands (e.g., warfarin) (Fig. 1). At pH greater than 8.0 and in the absence of ligands, HSA changes conformation leading to the B form, which is characterized by increased affinity for some other ligands (e.g., heme). According to linked functions [22], ligands that bind preferentially to one of the conformational states of HSA allosterically modulate the F $\leftrightarrow$ N $\leftrightarrow$ B transition [2, 16–18, 20, 21, 23, 24].

The multidomain structural organization makes HSA a model system to investigate how interdomain interactions could affect the folding/unfolding process [25–32]. With use of different experimental techniques to follow thermal or chaotropic denaturation of HSA, it has been observed that the HSA N state unfolds in two sequential steps, domain II unfolding before domain I (i.e., the heme binding domain) [29–31]. Although the guanidinium chloride (GnCl)-induced unfolding of HSA has been reported to proceed cooperatively without any detectable intermediate state in the absence of ligand(s) that would stabilize the intermediate state(s) [30, 32], it has been suggested by Rezaei-Tavirani [31] that reversible unfolding of the HSA N form might occur through the formation of an intermediate species, possibly a molten globule, which could retain the ability to bind the heme. A similar mechanism has been proposed for the urea-induced reversible unfolding of the HSA F state [30].

Here, we report the GnCl-dependent heme–HSA reversible unfolding in the absence and presence of myristate, followed by NMR relaxometric measurements, circular dichroism (CD), and absorption spectroscopy. NMR relaxometry has been used recently to investigate the effect of prototypic drugs (such as ibuprofen and warfarin) on reversible heme–HSA unfolding, and has turned out to be a powerful technique to investigate protein structural changes in the proximity of a paramagnetic probe molecule (i.e., heme) [32]. Results obtained by NMR relaxation, CD, and absorption spectroscopy indicate that heme–HSA partially unfolds, in the presence of 1.0 M GnCl and 6 equiv of myristate, through the formation of a folding intermediate characterized by increased relaxivity and negative ellipticity in the Soret region. Further, the thermodynamics of

heme binding to HSA, in the absence and presence of GnCl and myristate, indicates that myristate stabilizes a folding intermediate state displaying heme affinity similar to that of native HSA.

Materials and methods

All reagents (from Sigma-Aldrich, St Louis, MO, USA) were of the highest purity available and were used without further purification. HSA was FA-free and its concentration was determined by the Bradford assay [33]. The heme concentration was determined spectrophotometrically at 535 nm after converting hemin to the heme–bisimidazolate derivative in sodium dodecyl sulfate micelles ($\varepsilon_{535} = 14.5\ \mathrm{cm^{-1}\ mM^{-1}}$) [34]. Heme–HSA was prepared by adding the appropriate volume of the stock heme solution (i.e., 1.2×10^{-2} M heme in 1.0×10^{-1} M NaOH) to the 1.0×10^{-3} M HSA solution (1.0×10^{-1} M phosphate buffer, pH 7.0) to obtain a final heme–HSA concentration ranging between 5.0×10^{-6} and 1.0×10^{-3} M. The heme to HSA ratio ranged between 1:10 and 9:10. The excess of HSA ensured that the heme was bound to the HSA primary binding site only [11].

The 1.0×10^{-1} M myristate solution was prepared by adding 1.0×10^{-4} mol sodium myristate to 1.0 ml of 1.0×10^{-1} M NaOH. To dissolve the FA, the suspension was heated to 100 °C and stirred. An appropriate aliquot of the myristate solution was then mixed with 1.0×10^{-4} M heme–HSA to achieve the desired myristate concentration. Then, the heme–HSA–myristate complex was incubated for 1 h at room temperature under continuous stirring [13]. Lastly, the pH was adjusted to pH 7.0 by adding few microliters of 1.0×10^{-1} M HCl or 1.0×10^{-1} M NaOH.

The heme–HSA–GnCl stock solution (containing 5.0 M GnCl) was prepared by dissolving GnCl in the heme–HSA solution. Then, different volumes of the heme–HSA solution (in the absence and presence of the chaotropic agent) were mixed to obtain the desired GnCl concentration at a fixed heme–HSA concentration. GnCl-induced HSA unfolding is fully reversible under the experimental conditions reported in the present study [25–32]. Samples were incubated for 1 h before measurements. Lastly, the pH was adjusted to pH 7.0 by adding a few microliters of 1.0×10^{-1} M HCl or 1.0×10^{-1} M NaOH.

Water proton T_1 measurements at 0.04 MHz, pH 7.0, and 25.0 °C were performed with a Stelar Spinmaster-FFC fast field cycling relaxometer (Stelar, Mede, PV, Italy) with 16 experiments in four scans. Briefly, macroscopic magnetization is obtained by inserting the sample in a magnetic field of 2.35×10^{-1} T (corresponding to 10 MHz proton Larmor frequency), then the magnetic field is switched to 9.4×10^{-3} T (corresponding to 0.04 MHz proton Larmor frequency) for variable time. During this evolution interval the macroscopic magnetization changes with a time constant corresponding to the T_1 value at 0.04 MHz. At the end, the magnetic field is switched to 2.21×10^{-1} T (corresponding to a 9.4 MHz proton Larmor frequency) and the magnetization is converted into an observable NMR signal by a radiofrequency pulse at 9.4 MHz. The intensity of the signal is proportional to the magnetization at the end of the evolution interval [35]. The reproducibility in T_1 measurements was ±0.5% [11]. The temperature was controlled by a Stelar VTC-91 airflow heater and checked in the sample cavity with a mercury thermometer. The r_1 relaxivity values (i.e., the paramagnetic contributions to the solvent water longitudinal relaxation rate referenced to that of a 1.0×10^{-3} M concentration of the paramagnetic agent) were determined by subtracting from the observed relaxation rate (R_1^{obs}) the blank relaxation rate (R_1^{dia}) measured for the buffer solution at the experimental temperature [35–37]. The heme–HSA concentration was 1.0×10^{-4} M.

Reversible GnCl-induced unfolding data were analyzed according to Eq. 1 (modified from [38]):

$$r_1 = r_\infty + \left[r_0 + \frac{\Delta r \times [\mathrm{GnCl}]}{K_d + [\mathrm{GnCl}]}\right] \times \left[\frac{1}{1 + e^{\left(-\frac{\Delta G^0 - m \times [\mathrm{GnCl}]}{RT}\right)}}\right], \quad (1)$$

where r_∞ is the r_1 value observed at saturating GnCl concentration, r_0 is the r_1 value observed in the absence of GnCl, Δr is the r_1 increase associated with the first denaturation step, i.e., the formation of the folding intermediate state, ΔG^0 is the standard Gibbs free energy for the global unfolding process, and K_d is the protein–GnCl affinity constant. The coefficient m is proportional to the protein surface exposed to the solvent.

CD experiments were performed with a JASCO J710 spectropolarimeter (JASCO, Tokyo, Japan) in the far-UV region (190–250 nm), the near-UV region (250–310 nm), and the Soret region (350–450 nm): the heme–HSA concentration was 5.0×10^{-7}, 2.0×10^{-5}, and 1.0×10^{-4} M, respectively. The cell length was 1.0 mm. The buffer was 0.1 M phosphate pH 7.0. All spectra were the average of four measurements and were corrected by baseline subtraction. The myristate concentration was 6 times the HSA concentration; after addition of GnCl and/or myristate, solutions were incubated for 60 min at 25 °C.

Heme binding to HSA was investigated spectrophotometrically using an optical cell with 1.0-cm path length with use of a Cary 50 Bio spectrophotometer (Varian, Palo Alto, USA) in the UV–vis region (300–800 nm). In experiments carried out at different HSA concentrations, a small amount of the heme solution (about 1.2×10^{-2} M) was diluted in the optical cell in 1.0×10^{-1} M phosphate

buffer, 10% dimethyl sulfoxide, pH 7.0, to a final chromophore concentration of 1.0×10^{-5} M. Then, small amounts of 1.0×10^{-3} M HSA were added to the heme solution and the absorption spectra were recorded after incubation for a few minutes after each addition. The same experiments were performed in the presence of 1.8×10^{-4} M myristate, 1.0 M GnCl, or both. Spectra were normalized with respect to the first spectrum. In experiments carried out at different heme concentrations, a small amount of the HSA solution (about 1.0×10^{-3} M) was diluted in the optical cell in 1.0×10^{-1} M phosphate buffer, 10% dimethyl sulfoxide, 1.0 M GnCl, pH 7.0, to a final HSA concentration of 1.0×10^{-5} M, in the absence and in the presence of 6.0×10^{-5} M myristate. Then, small aliquots of 1.2×10^{-2} M heme were added to the HSA solution and the absorption spectra were recorded after incubation for a few minutes after each addition. In parallel, spectra were recorded in the absence of HSA and pairwise subtracted from the first ones. In both cases, the binding isotherms were analyzed by plotting the difference of absorbance (ΔA) at 410 nm as a function of the HSA or heme concentration. Data were analyzed according to Eq. 2 (modified from [20]):

$$Y = \frac{\left(K_d^{-1}L_t + P_tK_d^{-1} + 1\right) - \sqrt{\left(K_d^{-1}L_t + P_tK_d^{-1} + 1\right)^2 - 4K_d^{-2}L_tP_t}}{2K_d^{-1}L_t}, \quad (2)$$

where Y is the molar fraction of bound heme, K_d is the dissociation equilibrium constant of heme–HSA formation, L_t is the total ligand (i.e., heme) concentration, and P_t is the total protein (i.e., HSA) concentration.

The three-dimensional structures of HSA in the absence and in the presence of heme and myristate were downloaded from the Protein Data Bank (entries 1AO6 and 1O9X, respectively) [13, 39]. Structural models were drawn with the UCSF Chimera package from the Resource for Biocomputing, Visualization, and Informatics at the University of California, San Francisco [40].

Results

Figure 2 shows the GnCl-induced reversible unfolding of heme–HSA followed by measuring the millimolar relaxivity r_1 at 0.04 MHz, pH 7.0, and 25 °C. In the absence (see also [21]) and in the presence of 3 equiv of myristate with respect to total HSA (i.e., 3.0×10^{-3} M myristate), the r_1 value of the 1.0×10^{-4} M heme–HSA solution (in the presence of a tenfold excess of HSA, i.e., 1.0×10^{-4} M heme and 1.0×10^{-3} M HSA) decreases from 25 to 8 s^{-1} mM^{-1} on raising the GnCl concentration to 5.0 M. The denaturation curves are in agreement with a simple global unfolding process (Eq. 1, $\Delta R = 0$), from which ΔG^0 values of 6.4 ± 1.0 and 7.9 ± 1.0 kJ mol^{-1}, respectively, are derived (Table 1); furthermore, values of m (proportional to the increase of the protein surface exposed to the solvent on unfolding) of 4.4 ± 0.6 and 3.8 ± 0.4 kJ l mol^{-2}, respectively, were obtained. On the other hand, in the presence of 6 equiv of myristate (with respect to total HSA, i.e., 6.0×10^{-3} M myristate), the r_1 value of the 1.0×10^{-4} M heme–HSA solution (in the presence of a tenfold excess of HSA, i.e., 1.0×10^{-4} M heme and 1.0×10^{-3} M HSA) increases from 25 to 33 s^{-1} mM^{-1} on raising the GnCl concentration to 1.0 M. A further increase of the GnCl concentration from 1.5 to 5.0 M induces a reduction of r_1 values, which tend to the asymptotic value of 14 s^{-1} mM^{-1} at saturating denaturant concentrations. The analysis of data according to Eq. 1 allowed us to determine the dissociation equilibrium constant for the formation of the heme–HSA–myristate–GnCl complex (i.e., the species endowed with a high relaxivity value; $K_d = 0.3 \pm 0.2$ M, corresponding to a Gibbs free energy for the GnCl binding to HSA of

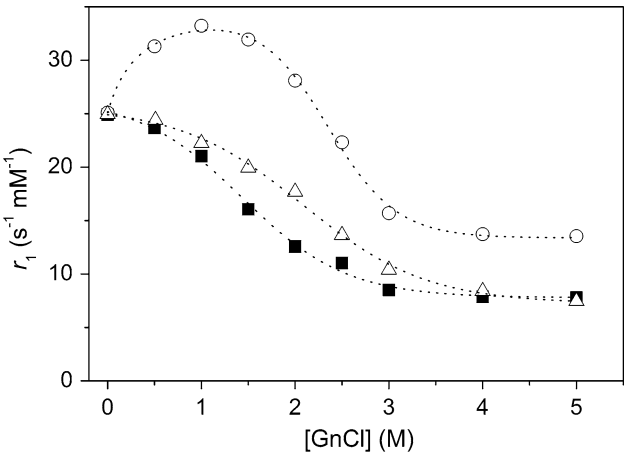

Fig. 2 Effect of guanidinium chloride (*GnCl*) on unfolding of heme–HSA in the absence of myristate (*squares*) and in the presence of 3 equiv (i.e., 3.0×10^{-3} M; *triangles*) and 6 equiv (i.e., 6.0×10^{-3} M; *circles*) of myristate, as obtained by measuring r_1 at 0.04 MHz proton Larmor frequency, pH 7.0, and 25 °C. The *dotted lines* were obtained by the analysis of data according to Eq. 1. For details, see the text and Table 1

Table 1 Thermodynamic parameters for global unfolding of heme–human serum albumin (heme–HSA)

Myristate (M)	ΔG^0 (kJ mol^{-1})	m (kJ l mol^{-2})
0	6.4 ± 1.0	4.4 ± 0.6
3.0×10^{-3} [a]	7.9 ± 1.0	3.8 ± 0.4
6.0×10^{-3} [b]	15.8 ± 3.2	6.8 ± 1.2

[a] Corresponding to 3 equiv of myristate per total HSA

[b] Corresponding to 6 equiv of myristate per total HSA

1.3 ± 0.5 kJ mol^{-1}), the Gibbs free energy for the global unfolding process (ΔG^0 = 15.8 ± 3.2 kJ mol^{-1}; see Table 1), and m (6.8 ± 1.2 kJ l mol^{-2}). The free energy for the global unfolding increases with the myristate concentration, thus suggesting a stabilizing effect of myristate; on the other hand, m remains mostly unaffected at low myristate concentration, whereas it shows a twofold increase in the presence of 6 equiv of myristate (Table 1). The myristate concentration corresponding to 6 equiv is 6.0 × 10^{-3} M, i.e., higher than the critical micellar concentration (4.5 × 10^{-3} M). This is not a concern when the protein is folded, as myristate is completely bound to HSA, whereas myristate micelles are formed when the protein is denatured and myristate is released. For this reason the asymptotic value for r_1 of free heme in the presence of 6.0 × 10^{-3} M myristate is different from the values measured in the presence of 3.0 × 10^{-3} M and in the absence of myristate.

The peculiar relaxivity enhancement observed in Fig. 2 prompted us to characterize structural changes associated with myristate binding and GnCl-induced denaturation by CD. Figure 3 shows the CD spectra of heme–HSA in the Soret region (350–450 nm), in the near-UV region (250–310 nm), and in the far-UV region (190–250 nm). Similarly to what was observed for classic heme–proteins (e.g., myoglobin) [40, 41], molar ellipticity measured in the Soret region reaches its maximum value 24 h after heme addition, showing a slow correct positioning of the prosthetic group [42]. The inspection of CD spectra obtained under the same experimental condition indicates that the secondary structure of HSA is quite unaffected by heme binding and only minor rearrangements are observed in the aromatic pattern (data not shown). As can be derived from Fig. 3a, myristate binding dramatically increases the heme ellipticity with an absolute 1.4–1.5-fold change without changes in peak wavelength and spectrum shape. This result may indicate a stabilization of the heme–protein complex and/or an increased hydrophobicity of the heme pocket. Remarkably, the addition of 1.0 M GnCl in the presence of myristate only slightly reverses the effect induced by myristate binding, keeping the ellipticity still more negative than in the absence of both GnCl and myristate. On the other hand, in the absence of myristate, the addition of 1.0 M GnCl clearly destabilizes the heme–protein complex (as indicated by the decrease of the negative ellipticity, see Fig. 3a) and 5.0 M GnCl leads to a complete denaturation. Near-UV CD spectra of heme–HSA (Fig. 3b) display a low ellipticity, mostly referable to Tyr residues, due to the presence of only a single Trp residue in HSA [2]. Separate addition of either 1.0 M GnCl or 6 equiv of myristate does not induce significant changes in the features of the spectrum except (in the case of myristate) for some broadening of Trp peaks and slight changes in the Phe-Tyr zone (i.e., over the 255–275 nm range). On the other hand, 6 equiv of myristate and 1.0 M GnCl together have a greater effect on the negative ellipticity decrease (Fig. 3b), indicating remarkable rearrangements in the protein tertiary structure that are better observed in the difference spectra reported in Fig. 3c. Addition of 5.0 M GnCl (in the presence or in the absence of 6 equiv of myristate) results in a destructured aromatic pattern for heme–HSA (Fig. 3b). In Fig. 3d the CD UV spectra of heme–HSA are shown. In the case of heme–HSA, addition of myristate only brings about a small decrease of ellipticity at 208 nm, leaving the Θ value at 222 nm unaffected (Fig. 3d, e), with a consequent decrease of the 208 to 222 nm ellipticity ratio. According to several authors [43, 44] changes of this ratio may reflect rearrangements of aromatic residues, in particular the Trp residue, possibly related to different tertiary constraints, as described above for CD measurements in the near-UV region. The overall secondary structure seems to be only slightly perturbed by separate addition of 1.0 M GnCl or 6 equiv of myristate and the same is observed when both are present. An almost complete denaturation is instead observed upon addition of 5.0 M GnCl in the absence or in the presence of 6 equiv of myristate, as suggested by the random-coil predominance (Fig. 3d).

To better characterize the heme–HSA species endowed with enhanced relaxivity, heme binding to HSA was monitored by optical spectroscopy in the presence of 1.8 × 10^{-4} M myristate (corresponding to 6 equiv of myristate or more in the whole HSA concentration range), and/or of 1.0 M GnCl. Titrations were performed both at fixed heme concentration by changing the HSA concentration and at fixed protein concentration by changing the heme concentration. In this way it is possible to discriminate simple binding equilibria from those involving multiple binding sites.

Figure 4 shows difference spectra and binding isotherms for heme binding to HSA as a function of the protein concentration in the absence of third components (i.e., GnCl and myristate) and in the presence of 1.0 M GnCl, 1.8 × 10^{-4} M myristate, or of both 1.0 M GnCl and 1.8 × 10^{-4} M myristate, at pH 7.0 and 25 °C. Data analysis according to Eq. 2 allowed us to determine values of K_d = 5.0 ± 0.02 × 10^{-7} M for heme binding to HSA in the absence of third components (i.e., GnCl and myristate). Heme binding to HSA in the presence of 1.8 × 10^{-4} M myristate displays a more complicated behavior, as expected on the basis of direct competition of myristate for the heme binding site and for the progressive removal of myristate when the HSA concentration increases [4, 5, 10, 20]. Similarly, heme binding to HSA in the presence of 1.0 M GnCl cannot be analyzed using a simple binding model, since the folded fraction, at high HSA

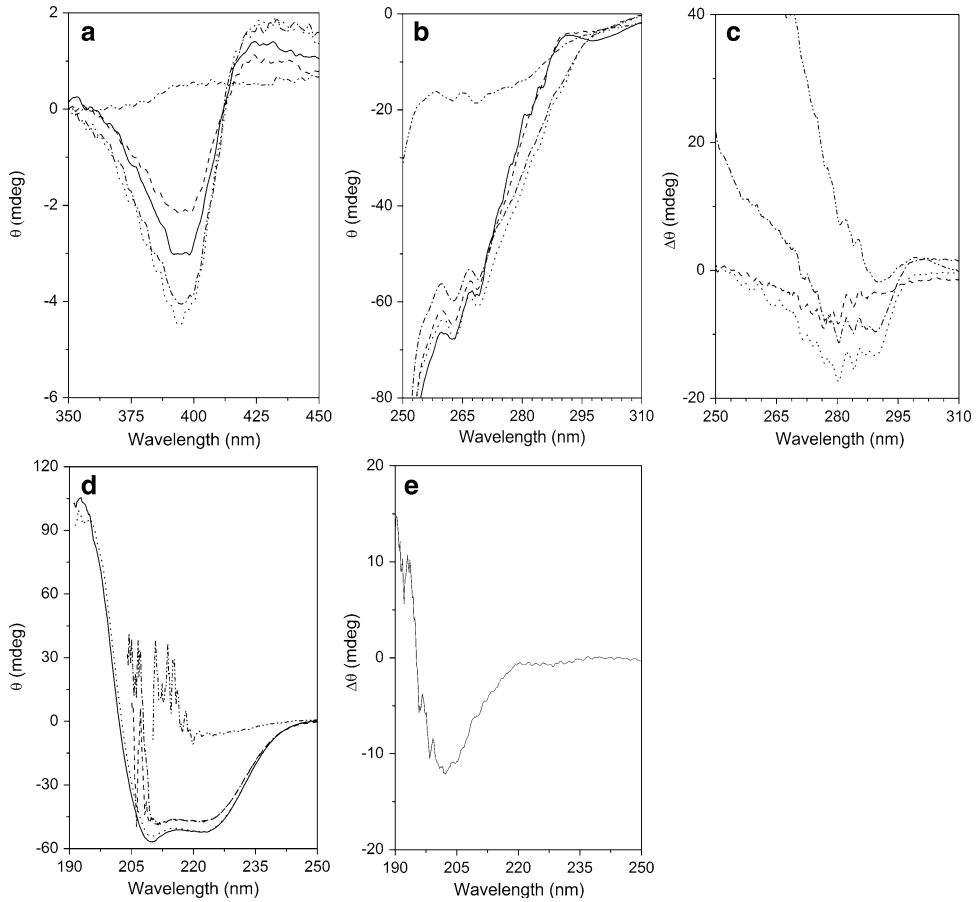

Fig. 3 Circular dichroism (CD) investigation of HSA and heme–HSA unfolding. **a** CD spectra in the Soret region of 1.0×10^{-4} M heme–HSA (i.e., 1.0×10^{-3} M HSA) in the absence of GnCl and myristate (*solid line*) and in the presence of 1.0 M GnCl (*dashed line*), 6.0×10^{-3} M myristate (*dotted line*), 1.0 M GnCl and 6.0×10^{-3} M myristate (*broken line with single dot*), and 5.0 M GnCl and 6.0×10^{-3} M myristate (*broken line with double dot*). **b** CD spectra in the near-UV region of 2.0×10^{-5} M heme–HSA (i.e., 2.0×10^{-4} M HSA) in the absence of GnCl and myristate (*solid line*) and in the presence of 1.0 M GnCl (*broken line*), 1.2×10^{-3} M myristate (*dotted line*), 1.0 M GnCl and 1.2×10^{-3} M myristate (*broken line with single dot*), and 5.0 M GnCl and 1.2×10^{-3} M myristate (*broken line with double dot*). **c** Difference spectra of 2.0×10^{-5} M heme–HSA (i.e., 2.0×10^{-4} M HSA) in the presence of 1.0 M GnCl (*broken line*), 1.2×10^{-3} M myristate (*dotted line*), 1.0 M GnCl and 1.2×10^{-3} M myristate (*broken line with single dot*), and 5.0 M GnCl and 1.2×10^{-3} M myristate (*broken line with double dot*) minus 2.0×10^{-5} M heme–HSA. **d** CD spectra in the far-UV region of 5.0×10^{-7} M heme–HSA (i.e., 5.0×10^{-6} M HSA) in the absence of GnCl and myristate (*solid line*) and in the presence of 1.0 M GnCl (*broken line*), 3.0×10^{-5} M myristate (*dotted line*), 1.0 M GnCl and 3.0×10^{-5} M myristate (*broken line with single dot*), and 5.0 M GnCl and 3.0×10^{-5} M myristate (*broken line with double dot*). **e** CD difference spectra of 5.0×10^{-7} M heme–HSA in the presence of 3.0×10^{-5} M myristate minus 5.0×10^{-7} M heme–HSA. All the CD measurements were performed in 0.1 M phosphate buffer pH 7.0, in a 1.0-mm cell at 25 °C. For details, see the text

concentration, could be enough to bind the heme. In the presence of both 1.0 M GnCl and 1.8×10^{-4} M myristate, the binding curve apparently assumes hyperbolic behavior, although an accurate quantitative analysis cannot be performed.

Figure 5 shows difference spectra and binding isotherms for heme binding to HSA as a function of the heme concentration in the presence of 1.0 M GnCl, both in the presence and in the absence of 6.0×10^{-5} M myristate. When the heme concentration is increased at fixed HSA, myristate, and GnCl concentration, a hyperbolic binding curve is observed [$K_d = (5.0 \pm 0.7) \times 10^{-6}$ M]. In contrast, when the heme concentration is increased at fixed HSA and GnCl concentration, in the absence of myristate, a smooth increase is observed, indicating a reduction of the binding affinity [$K_d = (7.1 \pm 0.3) \times 10^{-5}$ M].

Discussion

Heme spectroscopic properties allow the investigation of functional and structural aspects of heme-bound proteins by optical absorption spectroscopy, CD, and ^{1}H-NMR relaxometry [4, 35, 36, 45–47]. Relaxivity in heme–proteins

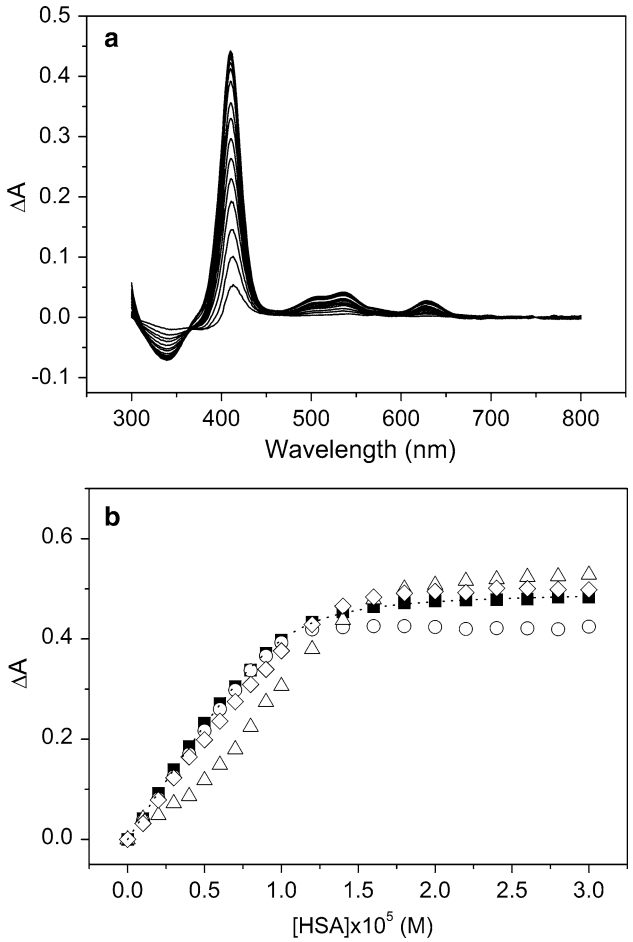

Fig. 4 Heme binding to HSA. **a** UV–vis difference spectra for a solution of 1.0×10^{-5} M heme titrated with HSA (0–3.0×10^{-5} M) in the absence of myristate and GnCl. **b** Titration of heme with HSA in the absence of myristate and GnCl (*squares*) and in the presence of 1.0 M GnCl (*triangles*), of 1.8×10^{-4} M myristate (*circles*), and of both 1.0 M GnCl and 1.8×10^{-4} M myristate (*diamonds*), pH 7.0 and 25 °C. The *dotted line* was obtained by the analysis of data according to Eq. 2. For details, see the text

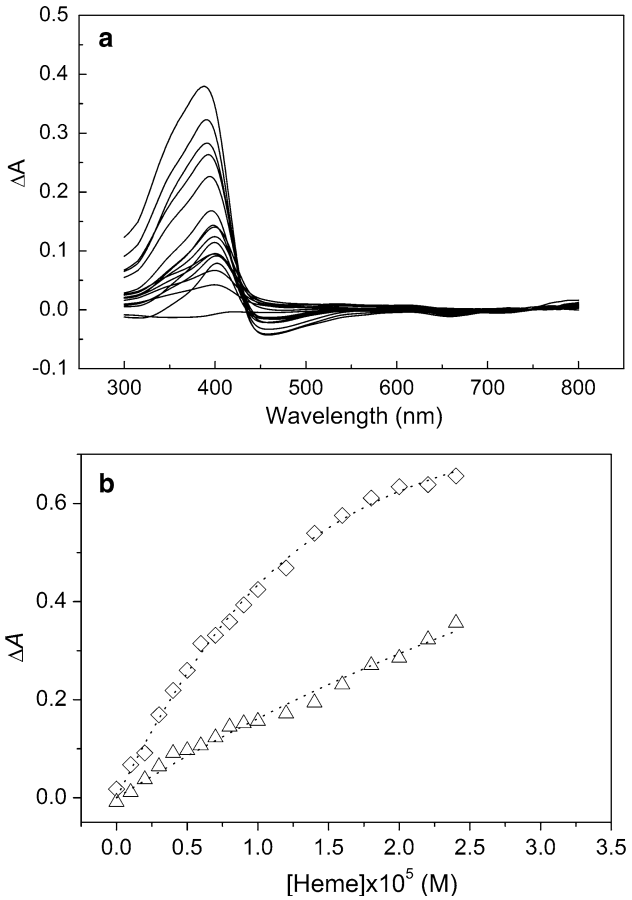

Fig. 5 Heme binding to HSA. **a** UV–vis difference spectra for a solution of 1.0×10^{-5} M HSA titrated with heme (0–2.5×10^{-5} M) in the absence of myristate and in the presence of 1.0 M GnCl. **b** Titration of HSA with heme in the presence of 1.0 M GnCl (*triangles*) and of both 1.0 GnCl and 6.0×10^{-5} M myristate (*diamonds*), pH 7.0 and 25 °C. The *dotted lines* were obtained by the analysis of data according to Eq. 2. For details, see the text

is usually due to second-sphere contributions, i.e., water molecules bound to the protein in the close proximity of a paramagnetic metal center and able to exchange with the bulk water [35–37]. Heme–HSA shows a considerably high r_1 value (approximately 25 s^{-1} mM^{-1}), compared with other heme–proteins such as hemoglobin and myoglobin [11, 19, 32, 48–51]. Nuclear magnetic relaxation dispersion studies of heme–HSA revealed a strong paramagnetic contribution due to a cluster of water molecules buried near the heme that may be employed to follow a number of events including conformational transitions [16]. Addition of GnCl up to 5.0 M brings about a progressive decrease of r_1 (Fig. 2), reflecting a denaturation process accompanied by the opening of the heme pocket and free exchange of water molecules between the bulk solution and the proximity of the paramagnetic center. The same pattern, though shifted toward somewhat higher GnCl concentrations, is observed in the presence of 3 equiv of myristate (Fig. 2), suggesting that a partial occupancy of the FA binding sites induces a modest stabilization of heme–HSA. Remarkably, r_1 is further increased in heme–HSA to approximately 33 s^{-1} mM^{-1} by increasing the GnCl concentration to 1.0 M in the presence of 6 equiv of myristate, corresponding to the full saturation of the FA binding sites (with the obvious exclusion of FA1, where heme is bound). The high r_1 value of the heme–HSA–myristate–GnCl complex could be related to the increase of the solvation in the proximity of the paramagnetic center, which occurs without losing most of the globular structure. Therefore, the formation of a partially relaxed structure could be envisaged as an intermediate along the heme–HSA–myristate unfolding pathway, likely accompanied by the expansion of the water-accessible internal volume of heme–HSA in the close proximity of the paramagnetic center, allowing an

increase of the number of second-sphere water molecules close to the heme [35–37]. At GnCl concentration higher than 1.5 M, the tertiary structure of heme–HSA unfolds and consequently the paramagnetic contribution is lost; thus, the complete unfolding of the heme–protein structure results in the release of the second-sphere water molecules that become free to diffuse into the solvent [11, 35–37]. As reported in Table 1, ΔG^0 values for the denaturation of heme–HSA are significantly dependent on the myristate concentration; although ΔG^0 values do not change after the addition of up to 3 equiv of myristate, the presence of 6 equiv of myristate brings about a remarkable stabilization of heme–HSA, as shown by the twofold ΔG^0 increase.

Altogether, these data provide solid support for the existence of a three-state unfolding pathway for HSA through the formation of a folding intermediate, in agreement with what was suggested by Santra et al. [28], who reported the existence of a folding intermediate with native-like secondary structure at GnCl concentrations lower than 1.5 M. This hypothesis is further strengthened by the analysis of the CD spectra in the Soret region, in the near-UV region, and in the far-UV region. This investigation indicates that myristate induces a dramatic conformational change(s) of the heme cavity, which becomes more compact upon addition of myristate, such that further addition of 1.0 M GnCl barely affects it. This structural transition of the heme pocket is essentially heme-independent, as shown by matching HSA and heme–HSA CD spectra, and it is accompanied only by minor rearrangement of Tyr residues (Fig. 3). On the other hand, more evident perturbations on the Trp residue in heme–HSA may suggest that myristate mainly affects structural contacts between different domains and stabilizes a folding intermediate state.

Independent proof of the occurrence of a folding intermediate in the denaturation of HSA in the presence of 6 equiv of myristate has been obtained by looking at the heme binding properties of HSA in the absence and in the presence of 1.0 M GnCl, of 1.8×10^{-4} M myristate, and of both 1.0 M GnCl and 1.8×10^{-4} M myristate, at pH 7.0 and 25 °C (Fig. 4b). In the presence of either GnCl or myristate, the binding isotherms deviate from hyperbolic behavior. In particular, in the presence of 1.0 M GnCl, the curve assumes a sigmoidal shape; this behavior could be accounted for by the fact that at high HSA concentration a significant protein fraction may be present in the folded state and consequently binds the heme with high affinity. Although this experiment indicates the stabilizing effect of 1.8×10^{-4} M myristate on the HSA structure in the presence of 1.0 M GnCl, we cannot provide any quantitative analysis of the binding curves, nor ascertain whether both heme and myristate are essential for the stabilization of the folding intermediate, or the folding intermediate is induced by heme binding. For this reason, the heme binding to HSA was measured as a function of the heme concentration at fixed HSA concentration in the presence of 1.0 M GnCl, in the presence and absence of 6.0×10^{-5} M myristate (Fig. 5b). Interestingly, heme binds to HSA in the presence of 1.0 M GnCl according to a simple association equilibrium, suggesting that the folding intermediate occurs even in the absence of the heme. Moreover, the heme affinity is increased by 1 order of magnitude in the presence of 6.0×10^{-5} M myristate, thus confirming that the folding intermediate is stabilized by FAs.

Conclusions

Although the occurrence of a folding intermediate in the unfolding of HSA upon extensive glycation or lowering of pH was previously reported [52, 53], this is the first evidence for a folding intermediate in heme–HSA stabilized by myristate binding. Moreover, it appears that heme binding is not crucial for the formation of the folding intermediate. Remarkably, the NMR relaxometric technique used here allows detection of the events occurring in the close proximity of the paramagnetic probe, i.e., involving domain I that binds the heme (Fig. 1).

Furthermore, the folding intermediate does not show any relevant alteration of the secondary structure, whereas significant tertiary structural changes can be detected, being accompanied by a stabilization of the heme–protein interactions. Altogether, these data indicate that domain I, which undergoes a relevant structural change (leading to a more compact heme–protein interaction), could represent the main driving structural element for the conformational changes which induce the formation of the HSA folding intermediate.

Acknowledgment The authors thank Giorgio Pariani for technical assistance. Grant MiUR FIRB RBNE03PX83 to M.C. is gratefully acknowledged.

References

1. Carter DC, Ho JX (1994) Adv Protein Chem 45:153–203
2. Peters T Jr (1996) All about albumin: biochemistry, genetics and medical applications. Academic Press, Orlando
3. Curry S (2002) Vox Sang 83:315–319
4. Fasano M, Curry S, Terreno E, Galliano M, Fanali G, Narciso P, Notari S, Ascenzi P (2005) IUBMB Life 57:787–796
5. Ascenzi P, Bocedi A, Notari S, Fanali G, Fesce R, Fasano M (2006) Mini Rev Med Chem 6:483–489
6. Spector AA (1975) J Lipid Res 16:165–179
7. Hamilton JA (2004) Prog Lipid Res 43:177–199
8. Simard JR, Zunszain PA, Ha CE, Yang JS, Bhagavan NV, Petitpas I, Curry S, Hamilton JA (2005) Proc Natl Acad Sci USA 102:17958–17963

9. Kragh-Hansen U, Watanabe H, Nakajou K, Iwao Y, Otagiri M (2006) J Mol Biol 363:702–712
10. Simard JR, Zunszain PA, Hamilton JA, Curry S (2006) J Mol Biol 361:336–351
11. Fasano M, Baroni S, Vannini A, Ascenzi P, Aime S (2001) J Biol Inorg Chem 6:650–658
12. Wardell MZ, Wang JX, Ho J, Robert J, Rüker F, Ruble J, Carter DC (2002) Biochem Biophys Res Commun 291:813–819
13. Zunszain PA, Ghuman J, Komatsu T, Tsuchida E, Curry S (2003) Struct Biol 3:6
14. Fasano M, Fanali G, Leboffe L, Ascenzi P (2007) IUBMB Life 59:436–440
15. Fasano M, Fanali G, Fesce R, Ascenzi P (2008) In: Bolognesi M, di Prisco G, Verde C (eds) Dioxygen binding and sensing proteins. Springer, Heidelberg, pp 121–131
16. Baroni S, Mattu M, Vannini A, Cipollone R, Aime S, Ascenzi P, Fasano M (2001) Eur J Biochem 268:6214–6220
17. Mattu M, Vannini A, Coletta M, Fasano M, Ascenzi P (2001) J Inorg Biochem 84:293–296
18. Fasano M, Mattu M, Coletta M, Ascenzi P (2002) J Inorg Biochem 91:487–490
19. Monzani E, Curto M, Galliano M, Minchiotti L, Aime S, Baroni S, Fasano M, Amoresano A, Salzano AM, Pucci P, Casella L (2002) Biophys J 83:2248–2258
20. Fanali G, Fesce R, Agrati C, Ascenzi P, Fasano M (2005) FEBS J 272:4672–4683
21. Fanali G, Bocedi A, Ascenzi P, Fasano M (2007) FEBS J 274:4491–4502
22. Wyman J Jr (1964) Adv Protein Chem 19:223–286
23. Yamasaki K, Maruyama T, Yoshimoto K, Tsutsumi Y, Narazaki R, Fukuhara A, Kragh-Hansen U, Otagiri M (1999) Biochim Biophys Acta 1432:313–323
24. Ascenzi P, Bocedi A, Notari S, Menegatti E, Fasano M (2005) Biochem Biophys Res Commun 334:481–486
25. Dill K, Alonso DOV, Hutchinson K (1989) Biochemistry 28:5439–5449
26. Kosa T, Maruyama T, Sakai N, Yonemura N, Yahara S, Otagiri M (1998) Pharm Res 15:592–598
27. Farruggia B, Rodriguez F, Rigatuso R, Fidelio G, Picò G (2001) J Protein Chem 20:81–89
28. Santra MK, Banerjee A, Krishnakumar SS, Rahaman O, Panda D (2004) Eur J Biochem 271:1789–1797
29. Santra MK, Banerjee A, Rahaman O, Panda D (2005) Int J Biol Macromol 37:200–204
30. Ahmad B, Ankita, Khan RH (2005) Arch Biochem Biophys 437:159–167
31. Rezaei-Tavirani M, Moghaddamnia SH, Ranjbar B, Amani M, Marashi SA (2006) J Biochem Mol Biol 39:530–536
32. Fanali G, Ascenzi P, Fasano M (2007) Biophys Chem 129:29–35
33. Bradford MM (1976) Anal Biochem 72:248–254
34. Boffi A, Das TK, Della Longa S, Spagnuolo C, Rousseau DL (1999) Biophys J 77:1143–1149
35. Koenig SH, Brown RDIII (1990) Progr NMR Spectrosc 22:487–567
36. Bertini I, Luchinat C (1986) NMR of paramagnetic molecules in biological systems. Benjamin/Cummings, Menlo Park
37. Banci L, Bertini I, Luchinat C (1991) Nuclear and electron relaxation. VCH, Weinheim
38. Pace CN (1986) Methods Enzymol 131:266–280
39. Sugio S, Kashima A, Mochizuki S, Noda M, Kobayashi K (1999) Protein Eng 12:439–446
40. Pettersen EF, Goddard TD, Huang CC, Couch GS, Greenblatt DM, Meng EC, Ferrin TE (2004) J Comput Chem 25:1605–1612
41. La Mar GN, Yamamoto Y, Jue T, Smith KM, Pandey RK (1985) Biochemistry 24:3826–3831
42. Santucci R, Ascoli F, La Mar GN, Pandey RK, Smith KM (1993) Biochim Biophys Acta 1164:133–137
43. Manning MC, Woody RW (1989) Biochemistry 28:8609–8613
44. Santucci R, Polizio F, Desideri A (1999) Biochimie 81:745–751
45. Ascenzi P, Bocedi A, Visca P, Altruda F, Tolosano E, Beringhelli T, Fasano M (2005) IUBMB Life 57:749–759
46. Myer YP, Pande A (1978) In: Dolphin D (ed) The porphyrins. Academic Press, New York, pp 271–322
47. Goto Y, Fink AL (1994) Methods Enzymol 232:3–15
48. Aime S, Dastrù W, Fasano M, Arnelli A, Castagnola M, Giardina B, Ascenzi P (1992) Clin Chem 38:2401–2404
49. Aime S, Fasano M, Paoletti S, Arnelli A, Ascenzi P (1995) Magn Reson Med 33:827–831
50. Aime S, Fasano M, Paoletti S, Cutruzzolà F, Desideri A, Bolognesi M, Rizzi M, Ascenzi P (1996) Biophys J 70:482–488
51. Fasano M, Baroni S, Aime S, Mattu M, Ascenzi P (2003) J Inorg Biochem 95:64–67
52. Muzammil S, Kumar Y, Tayyab S (1999) Eur J Biochem 266:26–32
53. Sattarahmady N, Moosavi-Movahedi AA, Ahmad F, Hakimelahi GH, Habibi-Rezaei M, Saboury AA, Sheibani N (2007) Biochim Biophys Acta 1770:933–942